



Multicolor green to orange-red emission of Tb³⁺ and Eu³⁺-codoped tellurite glasses: Eu³⁺ concentration and Tb³⁺ → Eu³⁺ energy transfer

M. E. Alvarez-Ramos¹ · J. Alvarado-Rivera² · F. Félix-Domínguez¹ · R. C. Carrillo-Torres¹ · R. Sánchez-Zeferino¹ · G. Saavedra-Rodríguez¹

Received: 14 October 2022 / Accepted: 14 December 2022 / Published online: 31 December 2022
© The Author(s), under exclusive licence to Springer-Verlag GmbH, DE part of Springer Nature 2022

Abstract

A series of the TeO₂-GeO₂-ZnO glass system was single and double doped with different Tb³⁺/Eu³⁺ ratios. Their luminescent and colorimetric properties were analyzed for possible use as phosphor materials in lighting devices. The characterization by X-ray diffraction and Raman spectroscopy verified the glassy nature of the fabricated samples. The luminescent properties of the doped glasses were analyzed by means of steady-state fluorescence and time-resolved spectroscopy. The Tb³⁺ excitation bands observed in the codoped samples while monitoring the 700 nm emission of Eu³⁺, as well as the shortening of Tb³⁺ lifetime in presence of europium indicated a Tb³⁺ → Eu³⁺ energy transfer, which main interaction type is electric dipole-dipole, according to Inokuti-Hirayama model. The Eu³⁺ → Tb³⁺ energy transfer also occurs in the samples but with lower efficiency. The CIE1931 chromaticity coordinates, upon different excitation wavelengths, show a multicolor tuning from green to orange-red due to the lanthanide concentration ratio and the Tb³⁺ → Eu³⁺ energy transfer process.

Keywords Tellurite glasses · Energy transfer · Photoluminescence · Europium · Terbium

1 Introduction

Optoelectronic devices like lasers, fiber amplifiers, displays devices, and light-emitting diodes (LEDs), among others, have been promoting research towards materials with good physical, stability, and chemical properties adequate to host rare-earth ions for the mentioned applications [1–6]. In several trivalent lanthanide ions, the absorption bands due to 4f–4f or 5d–4f transitions are located in the range of InGaN, GaN, and AlGaN (350–400 nm) near-ultraviolet LEDs (NUV-LEDs) that are compatible with solid-state lighting devices [7–9]. Depending on the target application, a single ion or a combination of two or three rare-earth ions are introduced in oxide glasses to obtain multicolor or white light emission, following the red (R), green (G), and blue (B) system, tailoring the concentration of the lanthanide ions [9, 10]. For example, Softys et al. [11] used a combination

of Dy³⁺ (blue, yellow), Tb³⁺ (green), and Eu³⁺ (red) ions in triply doped PbO-B₂O₃-Al₂O₃-WO₃ glasses, varying their concentrations, resulting in warm white light emission upon direct excitation of ⁶H_{15/2} → ⁴K_{17/2} transition of Dy³⁺ (390 nm) with the Dy³⁺ → Tb³⁺ → Eu³⁺ energy transfer process. In this respect, Tb³⁺ ions with a 4f⁸ configuration and its dominant green emission from ⁵D₄ → ⁷F₅ transition, upon NUV excitation, have been demonstrated to be a suitable donor for acceptor ions like Sm³⁺ and Eu³⁺ [6, 12, 13]. Jha et al. [12] work on Tb³⁺/Sm³⁺-doped ZnO-P₂O₅-BaO-TiO₂ glasses revealed that the single-doped glasses presented pure green and orange emission. In contrast, the emission of the codoped glasses is possibly tuned from yellowish green to warm white through the energy transfer mechanism from Tb³⁺ to Sm³⁺. Similarly, the combination of trivalent terbium and europium ions has also been studied in several host materials due to the capability to tune the emission over a wide range of visible light, because of the energy transfer process that occurs from terbium to europium ions [14–16]. Even though the emission tunability is a desirable phosphor property for light-emitting diodes or display applications, in the last decade, few reports evaluated the luminescent and colorimetric properties of Tb³⁺/Eu³⁺ double-doped glasses varying europium concentration. Among the

✉ M. E. Alvarez-Ramos
mario@alvarez.uson.mx

¹ Departamento de Física, Universidad de Sonora,
83000 Hermosillo, Sonora, Mexico

² CONACYT-Departamento de Física, Universidad de Sonora,
83000 Hermosillo, Sonora, Mexico

glass host materials where the effect of europium content have been studied are the aluminum-zinc-phosphates [14], fluorophosphate [16], borate [15, 17], fluorozirconate [17], germanate [18], multicomponent [19] glasses, and oxide and oxyfluoride glass-ceramics [20, 21]. Furthermore, the energy transfer mechanism has been exploited in these works to tune the global emission tonality. Given the amorphous nature of glasses, presenting short-range order, the spectroscopic characteristics of the trivalent lanthanide ions contained in them are determined by the local structure. According to Bocharova et al. [22], dopant ions in disordered solids can distribute randomly or with local concentration displacement. In this work, the authors found that the dopant distribution and the $Tb^{3+} \rightarrow Eu^{3+}$ energy transfer depend on the dopant concentration, as well as the glass structure and glass composition.

Gopi et al. [15] work on Tb^{3+}/Eu^{3+} -doped borate glasses showed that at small increments of Eu^{3+} dopant from 0.1 to 1.0 mol%, under a 464 nm excitation, can shift the emission from greenish-yellow to orange-red. Also, Loos et al. [17] reported that Tb^{3+}/Eu^{3+} pair exhibit a similar chromatic behavior in borate and fluorozirconate glasses, upon excitation of 376 nm and 486 nm, confirming that the energy transfer process is enhanced as europium concentration increases from 0.1 to 0.5 mol%. Meanwhile, Wileńska et al. [19] studied Tb/Eu-doped multicomponent glasses with the composition $AlF_3-TiO_2-40PbO-H_3BO_3-SiO_2$ obtaining green, yellow, and cold-white light emission at different $xEu-(1-x)Tb$ molar ratios while maintaining the total concentration of dopants below 1 mol%. de Queiroz et al. [16] increased the molar ratio of Tb^{3+}/Eu^{3+} up to 1.5 mol% in fluorophosphate glasses and studied their luminescent and chromatic properties varying the excitation wavelength between 355 and 360 nm. They evidenced that the emission tonality of the glasses lies in a broad region of the visible light, in the red, green, and blue regions. Raju et al. [23] only studied the photoluminescent properties of Tb^{3+} and Eu^{3+} single-doped $TeO_2-B_2O_3-CdO-Li_2O-AlF_3$ glasses up to concentrations of 1.25 mol%. It is worth mentioning that codoping tellurite glasses with Tb^{3+}/Eu^{3+} has not been studied in-depth for high europium molar concentration, performing time-resolved photoluminescence spectroscopy analysis. Regarding oxide glasses, those based on tellurium oxide (TeO_2) and germanium oxide (GeO_2) are amorphous materials with high thermal and chemical stability, mechanical resistance, low melting temperature, mid-IR transparency, and low phonon energies of 700 and 880 cm^{-1} , respectively, that are appropriate as hosts for photoluminescent trivalent rare-earth ions [1, 24–26]. GeO_2 is a natural glass former, while TeO_2 is a conditional glass former, which requires to be combined with other compounds like alkaline oxides, sulfides, fluorides or chlorides to form a stable glass [26–28]. GeO_2 improves the mechanical resistance of the matrix, as well as their thermal

and chemical stability because of the higher bond strength of Ge–O bonds than Te–O bonds [28, 29]. Lesniak et al. [30] reported that for $TeO_2-GeO_2:Eu^{3+}$ glasses, GeO_2 concentration influences the fluorescence intensity ratio of Eu^{3+} ions, the refractive index and phonon energy of the glasses. Zinc oxide is often used in combination with TeO_2 because it contributes to stability, mechanical resistance, and high concentration acceptance (up to 40 mol% of ZnO) of the glass matrix. The addition of ZnO causes a disruption of the Te–O–Te bonds forming Te–O[−] terminal bonds, with non-bridging oxygens, depolymerizing the TeO_2 network [31, 32]. The non-bridging oxygens, together with tellurium lone electron pairs, have been related to the capability of TeO_2 glass to accept and accommodate modifier cations and their optical properties [33]. Thus, we report a comprehensive analysis of the luminescent, photometric, and colorimetric characteristics of TeO_2-GeO_2-ZnO (TGZ) glasses impurified with trivalent terbium, europium, and both lanthanides, with emphasis on the high molar concentration of europium, while evaluating the effect of the $Tb^{3+} \rightarrow Eu^{3+}$ energy transfer on the color tuning of the global emission of the double-doped TGZ glasses, covering a wide range of europium concentrations from 0.5 to 2 mol%.

2 Experimental details

TGZ glasses with a composition of $(80-x-y)TeO_2-10GeO_2-10ZnO:xTb^{3+}, yEu^{3+}$ (mol%) were fabricated according to the previously reported methodology [32], using reagent grade oxides powders, $Eu(NO_3)_3 \cdot 5H_2O$ and $Tb(CO_3)_3 \cdot xH_2O$ that were acquired from Sigma-Aldrich. Table 1 presents mol% concentrations of the precursors and dopants used to synthesize the glasses. The obtained samples were cut and polished into $0.6 \times 0.6 \times 0.2$ cm blocks. The vibrational features of the glasses were studied through Raman spectroscopy using a Horiba LabRAM HR spectrometer equipped with a He–Ne laser ($\lambda = 632.8$ nm). Photoluminescence spectra were registered by a Fluorolog fluorometer using a 450 W ozone-free Xe lamp. The fluorescence decay times of the emission originated from Tb^{3+} and Eu^{3+} were obtained through pulsed excitation using an Opolette HE 355 LD + UVDM (~ 10 ns, pulse energy = 1.0 mJ), and the resulting fluorescence signal was analyzed with a Jobin–Yvon Triax 550 monochromator coupled to a Horiba Jobin–Yvon i-Spectrum Two ICCD.

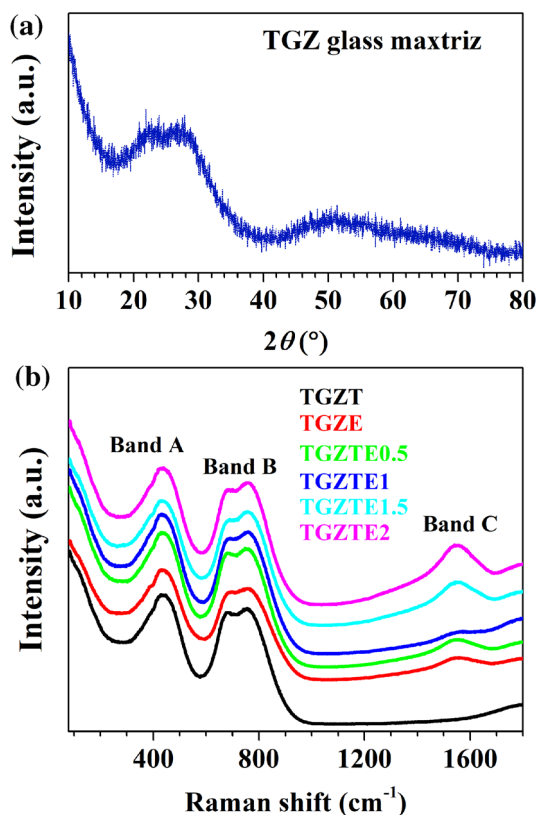
3 Results and discussion

3.1 X-ray diffraction and Raman spectroscopy

Figure 1a presents a representative diffractogram of the TGZ glasses. Three broad bands located around $2\theta = 22, 27,$ and

Table 1 Molar composition of the glass batches and labeling of the samples

Label	Composition (mol%)				
	(80-x-y) TeO ₂	GeO ₂	ZnO	x Tb(CO ₃) ₃ •xH ₂ O	y Eu(NO ₃) ₃ •5H ₂ O
TGZT	79.0	10	10	1.0	0
TGZE	79.0	10	10	0	1.0
TGZTE0.5	78.5	10	10	1.0	0.5
TGZTE1	78.0	10	10	1.0	1.0
TGZTE1.5	77.5	10	10	1.0	1.5
TGZTE2	77.0	10	10	1.0	2.0

**Fig. 1** a Representative diffraction pattern of TGZ glasses. b Raman spectra of the fabricated glasses, showing their characteristic bands

50 degrees can be distinguished, which are related to short-range order. The absence of well-defined diffraction peaks, within the diffractometer resolution, verifies the glassy structure of the sample.

Raman spectra of the fabricated TGZ glasses are displayed in Fig. 1b, showing the characteristic features of TeO₂-based glasses, which consist of two dominant bands. Band A extends from 300 to 600 cm⁻¹, while band B covers the 600–1000 cm⁻¹ range. Band C around 1550 cm⁻¹, can be observed in the glasses containing europium ions, and its origin is related to the presence of interstitial O₂ molecules due to the decomposition of the europium nitrate

hydrate [26]. The band at short wavenumbers is composed of the following vibrational features: Zn–O–Zn and Te–O–Zn bonds (380 cm⁻¹), O–Te–O in TeO₄ units (440 cm⁻¹), and Te–O–Te bridges (490 cm⁻¹) associated with network connectivity [32, 34–36]. Also, around ~450 cm⁻¹, a symmetric stretching vibration of Ge–O–Ge bonds in GeO₄ 4-membered rings can be found overlapped with the previously mentioned Te–O and Zn–O bond vibrations [37]. As for band B, three main vibrational features are present, which are the stretching modes of O–Te–O in TeO₄ (660 cm⁻¹), TeO₃₊₁ and [TeO₃]²⁻ (750 cm⁻¹), and short Te–O⁻ terminal bonds (820 cm⁻¹) with non-bonding oxygens (NBOs) [38]. Regarding germanium oxide, the anti-symmetric stretching vibrations of Ge–O–Ge bonds appear around 790 and 870 cm⁻¹, corresponding to the transverse and longitudinal optical split characteristic of GeO₂ [37]. It is worth mentioning that the TeO₂ vibrational modes dominate the Raman spectra, as it was previously reported for the TeO₂–GeO₂ binary glasses with contents below 20%mol [28]. In addition, there is still no conclusive evidence of the formation of a Te–O–Ge bond that could demonstrate the formation of mixed polyhedral units [28–30, 36]. However, Kalampounias et al. [28] reported that GeO₂ could act as a modifier, increasing the formation of TeO₃ units. A more insightful analysis of the glass structure through Raman spectra deconvolution analysis of europium-doped TGZ glasses and the TGZ matrix structural details were previously reported [38]. However, it was not possible to deconvolute the Raman spectra of TGZ glasses to evidence the bands related to germanium oxide polyhedra because they are completely overlapped with those of TeO₂.

3.2 Photoluminescence

The excitation spectrum of europium single-doped glass is presented in Fig. 2, it was obtained by monitoring the emission at 612 nm, related to ⁵D₀ → ⁷F₂ transition. It consists of several bands associated to parity-forbidden intra-4f transitions of Eu³⁺: ⁷F₀ → ⁵D₄ (365 nm), ⁷F₀ → ⁵L₁₀ (367 nm), ⁷F₀ → ⁵G_{2,3,4,5} (377 nm), ⁷F₀ → ⁵L₈ (383 nm), ⁷F₀ → ⁵L₇ (393 nm), ⁷F₁ → ⁵L₇ (400 nm), ⁷F₀ → ⁵D₃, ⁵L₆ (415 nm),

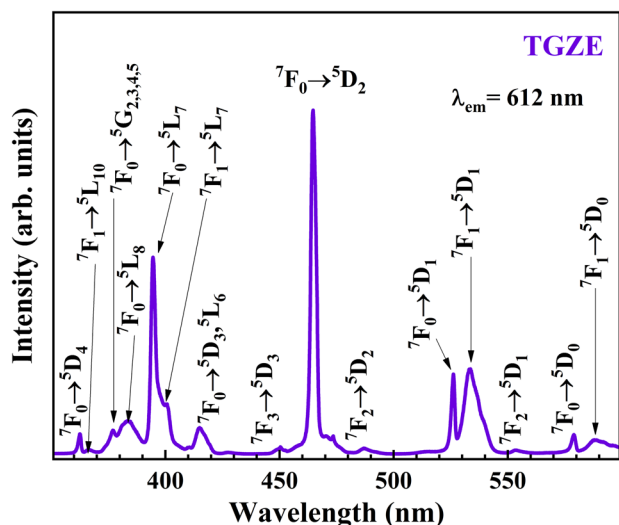


Fig. 2 Excitation spectrum of TGZE glass ($\lambda_{em} = 612$ nm)

${}^7F_3 \rightarrow {}^5D_3$ (449 nm) ${}^7F_0 \rightarrow {}^5D_2$ (465 nm), ${}^7F_2 \rightarrow {}^5D_2$ (487 nm), ${}^7F_0 \rightarrow {}^5D_1$ (525 nm), ${}^7F_1 \rightarrow {}^5D_1$ (532 nm), ${}^7F_2 \rightarrow {}^5D_1$ (553 nm), ${}^7F_0 \rightarrow {}^5D_0$ (578 nm), ${}^7F_1 \rightarrow {}^5D_0$ (588 nm) [39–41].

The photoluminescence spectrum of TGZE glass, obtained upon excitation at 393 nm (Fig. 3), consists of multiple bands assigned to intraconfigurational $4f^6 \rightarrow 4f^6$ transitions of europium ions from 5D_3 , 5D_2 , 5D_1 , and 5D_0 levels to the 7F_J manifold. The origin of these bands can be explained as follows: during the excitation, electrons are promoted from 7F_0 to 5L_6 level, from where they decay non-radiatively to the 5D_3 emitting level, and subsequently, to

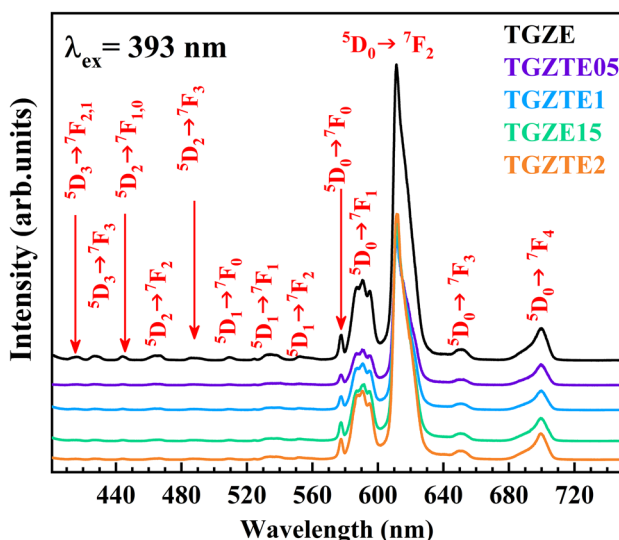


Fig. 3 Emission spectra of TGZE and codoped TGZTE0.5, TGZTE1, TGZTE1.5 and TGZTE2 glasses

the lower ${}^5D_{J=2,1,0}$ emitting levels, followed by a radiative decay towards the 7F_J levels. The same figure presents the emission spectra of TGZTE0.5, TGZTE1, and TGZTE1.5 and TGZTE2 glasses upon the same excitation wavelength.

In all samples, the most intense emission bands are the typical orange-red bands associated to the hypersensitive electric dipole ${}^5D_0 \rightarrow {}^7F_2$ transition, and the magnetic dipole ${}^5D_0 \rightarrow {}^7F_1$ transition, which is insensitive to the surrounding environment [35, 42, 43]. It is noticeable that the intensity of the blue-green bands decreases as the content of europium ions increases, while the intensity of the red bands is enhanced [34, 42, 43]. This phenomenon is due to an Eu → Eu energy transfer, through cross-relaxation processes, given that the energy difference associated to ${}^5D_3 \rightarrow {}^5D_2$ and ${}^5D_2 \rightarrow {}^5D_1$ is resonant with ${}^7F_0 \rightarrow {}^7F_4$ and ${}^7F_1 \rightarrow {}^7F_4$ transitions, according to the following possible mechanisms:

- (i) ${}^5D_3 + {}^7F_0 \rightarrow {}^5D_2 + {}^7F_4$
- (ii) ${}^5D_2 + {}^7F_1 \rightarrow {}^5D_1 + {}^7F_4$.

Due to the energy difference between 5D_1 and 5D_0 levels is only 1747 cm^{-1} , a multiphonon relaxation ${}^5D_1 \rightarrow {}^5D_0$ occurs, causing that the emissions from 5D_1 level to be negligible compared to those from the 5D_0 level [34, 42, 44].

The excitation spectrum of terbium single-doped glass (TGZT) is shown in Fig. 4. It was obtained by monitoring the emission at 543 nm and consists of multiple bands related to transitions from 7F_6 ground state to ${}^5G_2 + {}^5L_7 + {}^5L_8$, ${}^5L_9 + {}^5G_4$, ${}^5D_2 + {}^5G_5$, ${}^5L_{10}$, ${}^5G_6 + {}^5D_3$, and 5D_4 excited levels of Tb^{3+} , located at 342, 353, 358, 369, 378 and 485 nm, respectively, being the last one the most intense [45–48].

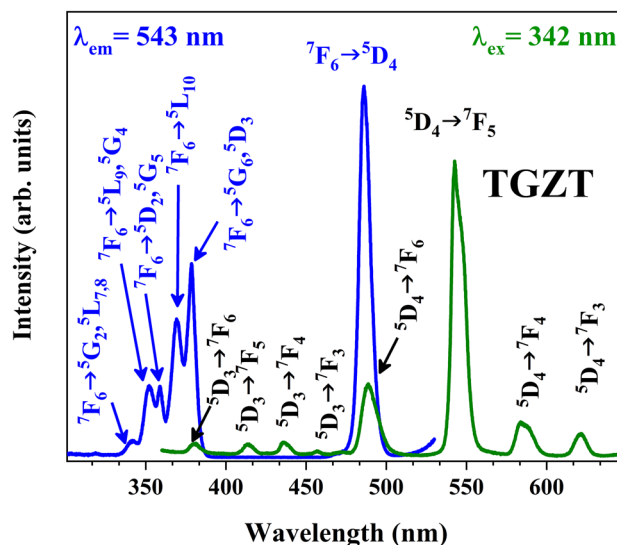


Fig. 4 Excitation spectrum of TGZT glass obtained by monitoring the emission of Tb^{3+} at 543 nm (blue line), and emission spectra acquired upon excitation of 342 nm (green line)

The emission of the TGZT glass, excited at 342 nm, is displayed in the same figure. It consists of four low intensity bands related to transitions from the ⁵D₃ level to ⁷F₆, ⁷F₅, ⁷F₄, ⁷F₃ levels, and four bands associated to transitions from ⁵D₄ level to ⁷F₆, ⁷F₅, ⁷F₄, and ⁷F₃ levels. The most intense emission band is the one associated to ⁵D₄ → ⁷F₅ transition giving origin to the characteristic bright green emission of Tb³⁺ ions.

3.3 Tb³⁺ → Eu³⁺ energy transfer

The effect of Eu³⁺ content in the codoped glasses was evaluated in a series of samples prepared varying the europium concentration from 0.5 to 2 mol% (TGZTE0.5, TGZTE1, TGZTE1.5, TGZTE2). The emission spectra of this samples, upon excitation of 342 nm, are presented in Fig. 5. This wavelength was selected because it does not excite Eu³⁺ ions (see Fig. 2) and it is resonant with ⁷F₆ → ⁵L₇ + ⁵G₂ + ⁵L₈ transitions of terbium ion. The luminescence results in the typical blue-green-red bands of 4f⁸ intra-configurational transitions of Tb³⁺ ion, from ⁵D₄ to ⁷F_J manifold, in addition to the characteristic orange-red emissions of Eu³⁺ ions, associated to ⁵D₀ → ⁷F_J transitions.

On the other hand, Fig. 6 depicts the excitation spectra of TGZE, TGZTE0.5, TGZTE1, TGZTE1.5, and TGZTE2 glasses, acquired while monitoring the emission at 700 nm, ⁵D₀ → ⁵F₄ transition of europium ions, where no Tb³⁺ emission exists. Two noteworthy features are present in this figure: first, the excitation bands associated to Eu³⁺ ions are dominant; and second, the presence of additional excitation bands which are related to terbium ions with maxima around 342, 366, 378, and 486 nm. It is worth mentioning

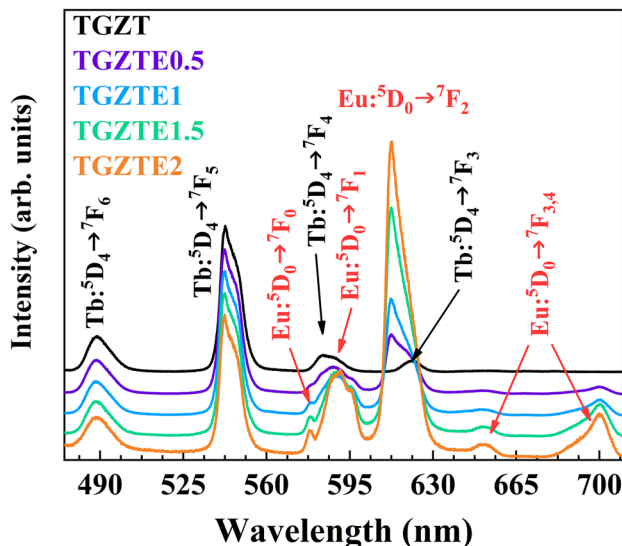


Fig. 5 Emission spectra of TGZT and codoped glasses excited at 342 nm

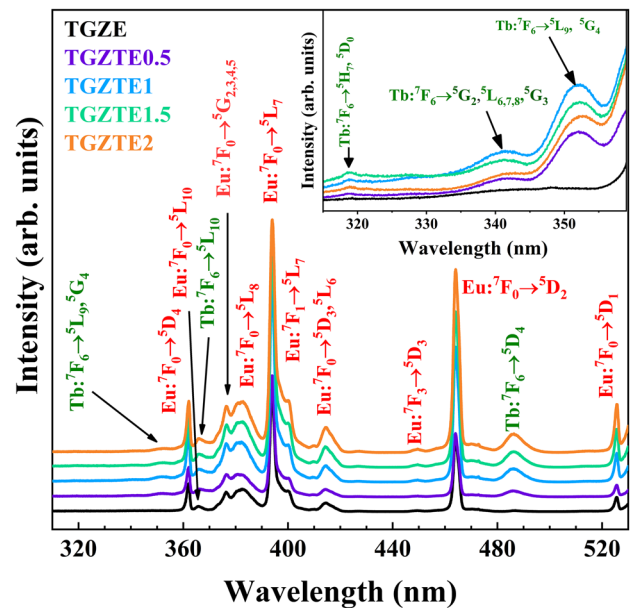


Fig. 6 Excitation spectra of TGZE, TGZTE0.5, TGZTE1, TGZTE1.5, and TGZTE2, monitored at 700 nm

the overlap of the excitation bands of both lanthanide ions at 366 nm and 378 nm; however, the excitation bands around 342 nm and 486 nm only correspond to terbium ion. Also, a decrease in intensity of the terbium excitation bands is observed when the concentration of europium ions increases from 0.5 to 2 mol% in the codoped samples (Fig. 7). Considering the spectral overlap between Tb³⁺ emissions (⁵D₄ → ⁷F₅ + ⁵D₄ → ⁷F₄) and Eu³⁺ excitation transitions (⁷F₁ → ⁵D₁, ⁷F₁ → ⁵D₀) depicted in Fig. 8, and the results

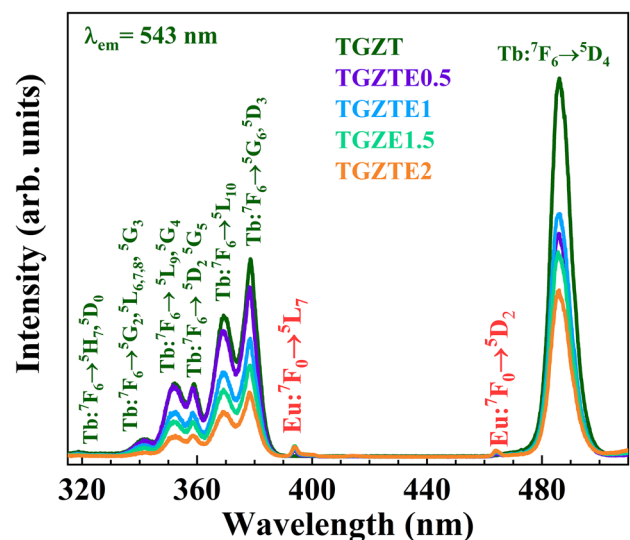


Fig. 7 Excitation spectra of TGZT and double-doped TGZ glasses monitoring Tb³⁺ emission at 543 nm

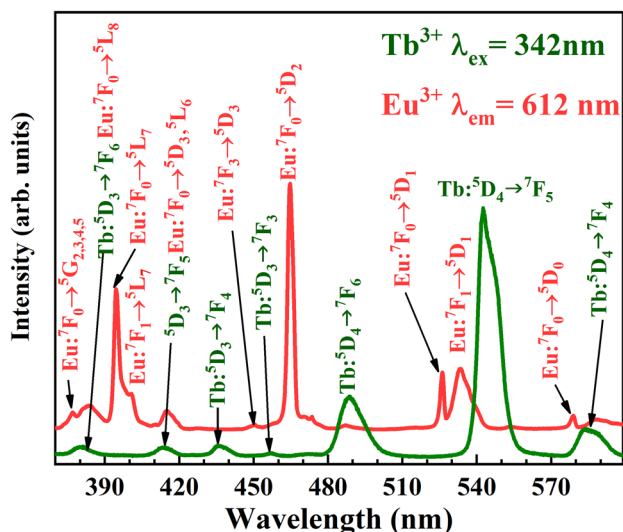


Fig. 8 Spectral overlap of TGZT glass emission spectra, acquired at 342 nm, and excitation spectra of TGZE recorded while monitoring the emission at 612 nm

mentioned above, it is possible to suggest that a $Tb^{3+} \rightarrow Eu^{3+}$ energy transfer process occurs in the codoped glasses, which could take place through the following three mechanisms, which are illustrated in the partial energy level diagram shown in Fig. 9 [45, 49]:

- (1) ${}^5D_3 [Tb^{3+}] + {}^7F_0 [Eu^{3+}] \rightarrow {}^7F_6 [Tb^{3+}] + {}^5G_{2,3,4,5}, {}^5L_8 [Eu^{3+}]$,
- (2) ${}^5D_3 [Tb^{3+}] + {}^7F_0 [Eu^{3+}] \rightarrow {}^7F_5 [Tb^{3+}] + {}^5D_3, {}^5L_6 [Eu^{3+}]$ and
- (3) ${}^5D_4 [Tb^{3+}] + {}^7F_1 [Eu^{3+}] \rightarrow {}^7F_4 [Tb^{3+}] + {}^5D_1 [Eu^{3+}]$.

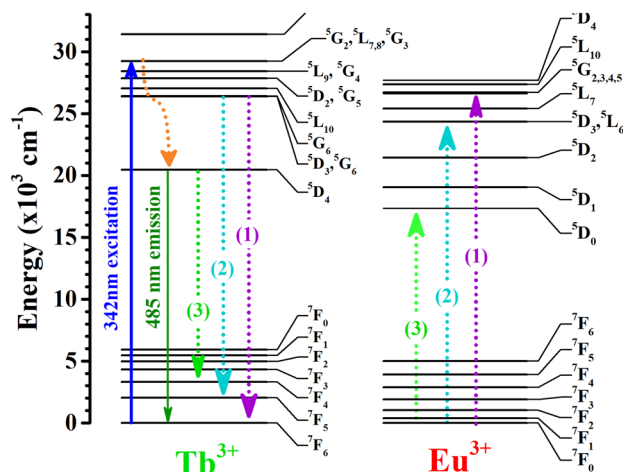


Fig. 9 Tb^{3+} and Eu^{3+} energy level diagrams depicting the $Tb^{3+} \rightarrow Eu^{3+}$ energy transfer process

To inquire further about the $Tb^{3+} \rightarrow Eu^{3+}$ energy transfer, time decay profiles of terbium ${}^5D_4 \rightarrow {}^7F_5$ transition (543 nm) were measured in the single-doped and codoped glasses. Tb^{3+} lifetimes were estimated by fitting the experimental data to an exponential function (Fig. 10a). The incorporation of Eu^{3+} in the terbium-doped glasses causes a reduction of the lifetime of the 543 nm emission, and this reduction is greater as the concentration of europium ions increases. This effect suggests a non-radiative energy transfer from Tb^{3+} to Eu^{3+} . The efficiency (η) and probability (P), of $Tb^{3+} \rightarrow Eu^{3+}$ energy transfer can be calculated by the following equations, respectively [50]:

$$\eta = 1 - \tau_{Tb \rightarrow Eu} / \tau_{Tb} \tag{1}$$

$$P_{Tb \rightarrow Eu} = 1 / \tau_{Tb \rightarrow Eu} - 1 / \tau_{Tb}, \tag{2}$$

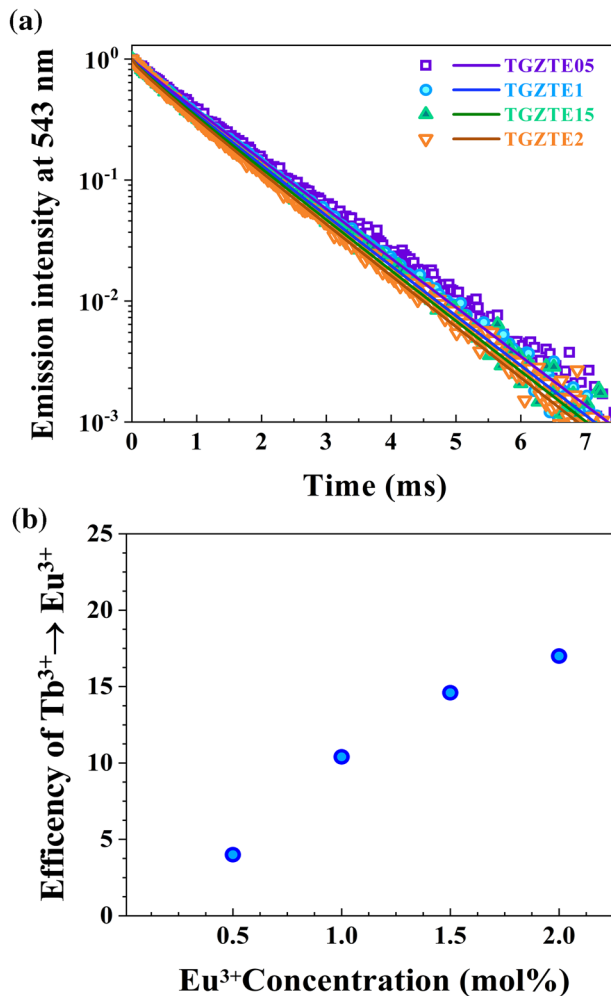


Fig. 10 **a** Measured decay times profiles of the 543 nm emission of Tb^{3+} in the codoped glasses; **b** efficiency of the $Tb^{3+} \rightarrow Eu^{3+}$ energy transfer process as a function of Eu^{3+} concentration

Table 2 Lifetimes of Tb³⁺ emission, and calculated values of efficiency and probability of the energy transfer process in TGZT and codoped glasses

Sample	τ (ms)	η (%)	P (s ⁻¹)
TGZT	1.086 ± 0.001	–	
TGZTE0.5	1.043 ± 0.001	4.0 ± 0.1	37.96 ± 1.01
TGZTE1	0.973 ± 0.001	10.4 ± 0.1	106.94 ± 1.93
TGZTE1.5	0.927 ± 0.001	14.6 ± 0.1	157.94 ± 2.12
TGZTE2	0.901 ± 0.003	17.0 ± 0.1	189.07 ± 3.69

where τ_{Tb} and $\tau_{\text{Tb-Eu}}$ are the Tb³⁺ lifetimes in the single-doped and codoped TGZ glasses, respectively. The decay times, efficiency, and probability values are enlisted in Table 2, showing that the efficiency of the process is improved, and its probability is bigger as the concentration of Eu³⁺ increases. The behavior of the efficiency of the energy transfer at different concentrations of Eu³⁺ is shown in Fig. 10b.

The Inokuti–Hirayama model (I–H model) [51] is appropriate to describe energy transfer processes where there is not fast energy transfer migration, and can be useful to determine the main mechanism involved in the Tb³⁺ → Eu³⁺ non-radiative energy transfer observed in the codoped glass samples. This model was applied to the temporal decay of the terbium emission ⁵D₄ → ⁷F₅ at 543 nm, considering multipolar interaction. The non-exponential curve of the temporal decay of the luminescence intensity, $I(t)$, can be written as follows:

$$I(t) = I_0 \exp \left[\left(\frac{-t}{\tau_0} \right) - \gamma_s \left(\frac{t}{\tau_0} \right)^S \right], \quad (3)$$

where I_0 denotes the intensity at $t=0$, τ_0 is the lifetime value of the donors (Tb³⁺) in the absence of Eu³⁺, γ_s is the energy transfer parameter, while the S value can take values of 6 (electric dipole–dipole), 8 (dipole–quadrupole), and 10 (quadrupole–quadrupole), depending on the multipolar interaction between the luminescent centers involved in the energy transfer process. In this way, the temporal behavior of ⁵D₄ → ⁷F₅ transition of Tb³⁺ under excitation at 342 nm, was fitted using Eq. (3) with $\tau_0 = 1.086$ ms, assuming different types of multipolar interactions. For all samples, the best fitting of the experimental data were obtained for $S = 6$, which infers that the Tb³⁺ → Eu³⁺ energy transfer process is dominated mainly by dipole–dipole interactions (Fig. 10a). Result that is similar to those observed in other Tb³⁺/Eu³⁺ codoped glasses [11, 45, 52]. The estimated energy transfer parameter γ_6 values obtained from the I–H model for TGZTE series of glasses are enlisted in Table 3. It is observed that the energy transfer parameter varies directly with Eu³⁺ concentration.

The critical interaction distance (R_c) for the energy transfer between both lanthanide ions can be calculated using the γ_6 parameter through the following equation [53]:

$$R_c = \left[\frac{3\gamma_6}{4\pi \cdot 1.77 \rho_{\text{Eu}}} \right]^{1/3}, \quad (4)$$

where ρ_{Eu} is the Eu³⁺ (acceptor) concentration. For the TGZTE glasses the ρ_{Eu} and R_c values are enlisted in Table 3.

The estimated critical interaction distances were found in 6.4–6.7 Å range for all TGZTE samples. Also, considering that ions are evenly distributed in the glass and under the assumption that they are confined in the interior of a sphere with radius R , the distance between a pair of randomly distributed ions (D_{random}) can be calculated using Eq. 5 [53]:

$$D_{\text{random}} = 2R = 2 \left(\frac{3}{4\pi \rho_T} \right)^{1/3}, \quad (5)$$

where ρ_T is the total ion concentration (Tb³⁺ plus Eu³⁺). The estimated D_{random} values are between 20 and 18 Å (see Table 3). Since the obtained R_c values are considerably shorter than the estimated interaction distance between a randomly distributed pair of ions, it is possible to suggest that the Tb³⁺ → Eu³⁺ energy transfer takes place inside clusters, instead of randomly located ions in TGZ glasses.

3.4 Eu³⁺ → Tb³⁺ energy transfer

In the Tb³⁺ excitation spectra shown in Fig. 7, the presence of two small excitation bands can be distinguished around 393 nm and 465 nm, that are associated to ⁷F₀ → ⁵L₆ and ⁷F₀ → ⁵D₂ transitions of europium ion, respectively. This fact indicates that the Eu³⁺ → Tb³⁺ energy transfer also takes place. To get a better insight about this process, the decay times of the 700 nm emission of Eu³⁺ (⁵D₀ → ⁵F₄ transition) in the codoped glasses were compared to the lifetimes of a TGZ series glasses single doped with 0.5, 1.0, 1.5 and 2 mol% of Eu³⁺: 1.119 ms (TGZE0.5), 1.084 ms (TGZE1.0), 1.054 ms (TGZE1.5) and 1.056 ms (TGZE2.0). According to the estimated results, the Eu³⁺ → Tb³⁺ energy transfer in the codoped glasses occurs

Table 3 Multipolar interaction parameter (γ_6), Eu³⁺ concentration (ρ_{Eu}), critical interaction distance (R_c), and distance between two randomly distributed ions (D_{random})

Sample	γ_6	ρ_{Eu} (ions/cm ³)	R_c (Å)	D_{random} (Å)
TGZTE0.5	0.0567	2.74×10^{19}	6.6	22
TGZTE1	0.1312	5.45×10^{19}	6.7	21
TGZTE1.5	0.1776	8.13×10^{19}	6.5	18
TGZTE2	0.2294	1.078×10^{20}	6.4	17

less efficiently, which is demonstrated by small variation of Eu^{3+} decay times, as well as their calculated efficiency and probability (Table 4). As can be noted, the presence of Tb^{3+} in the codoped glasses reduces the lifetime of the 700 nm emission, compared to the value obtained in the TGZE samples. However, this reduction may also be due to a cross-relaxation process between the europium ions, as described above.

Table 4 Decay times, efficiency, and probability values of $\text{Eu}^{3+} \rightarrow \text{Tb}^{3+}$ energy transfer in the double-doped glasses

Sample	τ (ms)	η (%)	P (s^{-1})
TGZTE0.5	1.069	4.47	41.80
TGZTE1	1.061	2.12	20.00
TGZTE1.5	1.052	0.19	1.80
TGZTE2	1.055	0.09	0.89

3.5 Photometric analysis

The tellurite glasses studied in this paper can find application as multicolor phosphor materials, given its wide range of tunability, from green to orange-red, by modifying the lanthanide concentration ratio or the excitation wavelength. To evaluate this tuning property, the fabricated glasses were excited in the UV range using different wavelengths and the chromaticity coordinates of their emission were estimated and plotted in the CIE 1931 chromaticity diagram (Fig. 11). Additionally, the correlated color temperature was calculated by means of McCamy equation [54]:

$$\text{CCT} = -449n^3 + 3525n^2 - 6823.8n + 5520.33, \quad (6)$$

where $n = (x - 0.3320)/(y - 0.1858)$, being x and y the chromaticity coordinates. The global emission of the glasses can be modulated from green to red region, passing through the yellow and orange regions of the spectrum, by simply modifying the $\text{Eu}^{3+}/\text{Tb}^{3+}$ ratio or the excitation wavelength

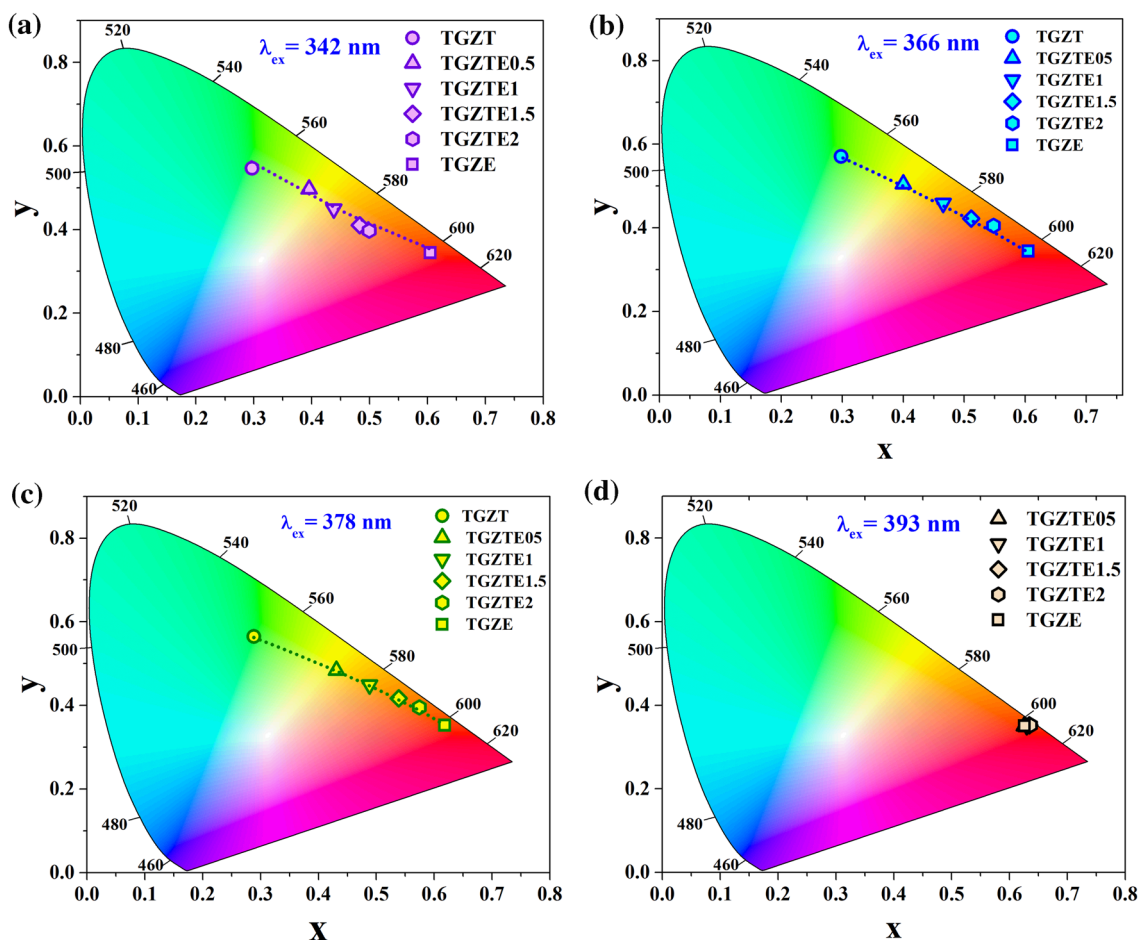


Fig. 11 CIE 1931 chromaticity coordinates of the global emission of the fabricated glasses, excited at different UV wavelengths using a xenon arc lamp, **a** 342 nm, **b** 366 nm, **c** 378 nm, and **d** 393 nm

(342, 366, 378, and 393 nm). The calculated chromaticity coordinates, CCT and color purity (CP) values are summarized in Table 5.

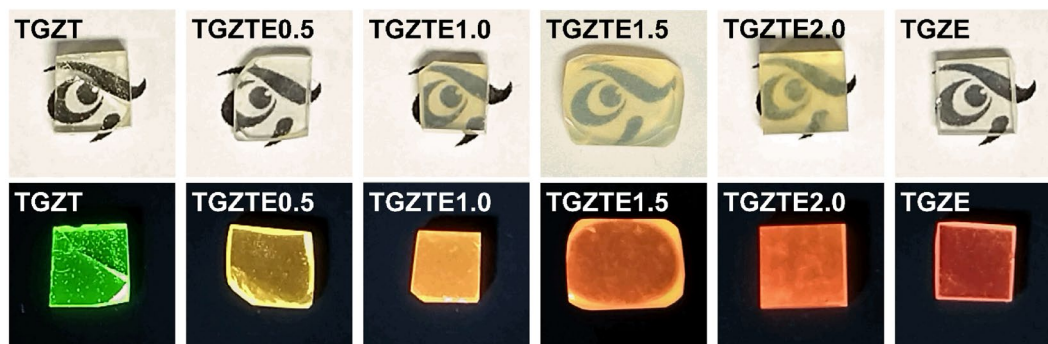
When the codoped samples are excited upon 342 nm (where europium ions do not have excitation band), the corresponding emission arises from the bands associated with both Tb³⁺ and Eu³⁺ ions, because the Tb³⁺ → Eu³⁺ energy transfer process. Besides, the increase of europium concentration and the consequent decrease of terbium emissions causes a shift of the global emission tonality towards the orange region (Fig. 11a). In the case of the values shown in Fig. 11b, c, the tunability of the global emission arises from the direct excitation of both ions and

the energy transfer process. Figure 12 shows photographs of the glasses under UV-LED light excitation of 365 nm, evidencing the emission color change of the single and codoped glasses from green to reddish-orange. Excitation wavelengths of 366 nm and 378 nm are resonant with ⁷F₆ → ⁵L₁₀, ⁵G₆, ⁵D₃ transitions of Tb³⁺ and ⁷F₀ → ⁵D₄, ⁷F₀ → ⁵L₁₀, ⁷F₀ → ⁵G_{2,3,4,5} transitions of Eu³⁺. Then, the origin of europium emission bands is due, first, to direct excitation of the Eu³⁺ and second to the Tb³⁺ → Eu³⁺ energy transfer process. Finally, when the glasses are excited at 393 nm, the double-doped glasses emission tonality comes fundamentally from europium ions in the reddish region, as shown in Fig. 11d.

Table 5 CIE 1931 chromaticity coordinates, CCT and CP values of the single and codoped TGZ glasses at different excitation wavelengths

Excitation wavelength		TGZT	TGZTE0.5	TGZTE1.0	TGZTE1.5	TGZTE2.0	TGZE
342 nm	x	0.2968	0.3954	0.4381	0.4830	0.4992	0.6046
	y	0.5470	0.4969	0.4493	0.4104	0.3975	0.3451
	CCT	6218	4273	3316	2389	2109	1917
	CP (%)	60	71	70	72	73	87
366 nm	x	0.2978	0.4000	0.4653	0.5113	0.5481	0.6046
	y	0.5711	0.5051	0.4587	0.4222	0.4052	0.3451
	CCT	6154	4223	2976	2177	1790	1916
	CP (%)	66	75	80	82	88	87
378 nm	x	0.2883	0.4310	0.4883	0.5385	0.5743	0.6182
	y	0.5652	0.4840	0.4490	0.4170	0.3953	0.3532
	CCT	6354	3627	2617	1918	1649	1914
	CP (%)	62	77	84	93	97	92
393 nm	x	–	0.6257	0.6297	0.6341	0.6365	0.6257
	y	–	0.3506	0.3515	0.3521	0.3524	0.3506
	CCT	–	2013	2035	2065	2082	2013
	CP (%)	–	96	95	96	97	94

Under daylight



Under UV-light excitation

Fig. 12 Photographs of the single and codoped glasses physical appearance under daylight (upper line) and their emission color under a 365 nm UV-LED light excitation (bottom line)

4 Conclusions

Tb³⁺, Eu³⁺ single-doped and Tb³⁺/Eu³⁺ codoped TeO₂-GeO₂-ZnO glasses were successfully prepared by melt quenching technique. The luminescent properties investigated upon UV excitation allowed to identify the presence of a Tb³⁺ → Eu³⁺ energy transfer process in the codoped samples. In such samples, the emission from terbium ⁵D₄ level decays faster than in TGZT (Tb³⁺-doped glass), revealing that Tb³⁺ can sensitize Eu³⁺ through non-radiative energy transfer. The fitting of the Tb³⁺ luminescence decay profile using the Inokuti-Hirayama model, allow us to infer that the Tb³⁺ → Eu³⁺ energy transfer process can be dominated by an electric dipole-dipole interaction in all codoped glasses. Furthermore, an increase of the energy transfer efficiency was observed, coupled with an enhancement of the Eu³⁺ emission at the expense of reducing the characteristic emission of Tb³⁺, as the Eu³⁺ concentration increases. The photometric characterization of Tb³⁺-Eu³⁺-doped glasses was carried out at different excitation wavelengths by evaluating the CIE 1931 chromaticity coordinates, showing a multicolor tuning of the emission from green to the orange-red region as a function of europium concentration with high color purity. Thus, the glasses under study can be good candidates as multicolor phosphors for their emission color tuning capability for solid-state devices.

Acknowledgements The authors thank to Consejo Nacional de Ciencia y Tecnología (CONACyT) for their support from project Cátedra-CONACyT 1959.

Author contributions All authors contributed to the study conception and design. Material preparation, data collection, analysis and editing were performed by JA-R, GS-R, RCC-T, FF-D and RS-Z. The first draft of the manuscript was written by MEA-R and all authors commented on previous versions of the manuscript. All authors read and approved the final manuscript.

Data availability The datasets generated during and/or analyzed during the current study are available from the corresponding author on reasonable request.

Declarations

Conflict of interest The authors declare there is no conflicts of interest.

References

1. K. Siva Rama Krishna Reddy, K. Swapna, Sk. Mahamuda, M. Venkateswarlu, A.S. Rao, G. Vijaya Prakash, Investigation on structural and luminescence features of Dy³⁺ ions doped alkaline-earth boro tellurite glasses for optoelectronic devices. *Opt. Mater.* **85**, 200–210 (2018). <https://doi.org/10.1016/j.optmat.2018.08.057>
2. H. Cankaya, A.T. Gorgulu, A. Kurt, A. Speghini, M. Bettinelli, A. Sennaroglu, Comparative spectroscopic investigation of Tm³⁺ tellurite glasses for 2-μm lasing applications. *Appl. Sci.* **8**, 333 (2018). <https://doi.org/10.3390/app8030333>
3. Y. Zhou, J. Chen, O.M. Bakr, H.T. Sun, Metal-doped lead halide perovskites: synthesis, properties, and optoelectronic applications. *Chem. Mater.* **30**, 6589–6613 (2018). <https://doi.org/10.1021/acs.chemmater.8b02989>
4. J. Rajagukguk, J. Kaewkhao, M. Djamal, R. Hidayat, S.Y. Ruangtawee, Structural and optical characteristics of Eu³⁺ ions in sodium-lead-zinc-lithium-borate glass system. *J. Mol. Struct.* **1121**, 180–187 (2016). <https://doi.org/10.1016/j.molstruc.2016.05.048>
5. R. Priyanka, S. Arunkumar, R.M. Ch Basavapoornima, K.M. Mathelane, Structural and spectroscopic investigations on Eu³⁺ ions doped boro-phosphate glasses for optical display applications. *J. Lumin.* **220**, 116964 (2020). <https://doi.org/10.1016/j.jlumin.2019.116964>
6. Y. Chen, G. Chen, X. Liu, J. Xu, T. Yang, C. Yuan, C. Zhou, Down-conversion luminescence and optical thermometric performance of Tb³⁺/Eu³⁺ doped phosphate glass. *J. Non-Cryst. Solids* **484**, 111–117 (2018). <https://doi.org/10.1016/j.jnoncrysol.2018.01.027>
7. Y. Muramoto, M. Kimura, S. Nouda, Development and future of ultraviolet light-emitting diodes: UV-LED will replace the UV lamp. *Semicond. Sci. Technol.* **29**, 4 (2014). <https://doi.org/10.1088/0268-1242/29/8/084004>
8. M. Kneissl, A brief review of III-nitride UV emitter technologies and their applications, in *III-nitride ultraviolet emitters*. ed. by M. Kneissl, J. Rass (Springer International Publishing, 2016), pp.1–7. https://doi.org/10.1007/978-3-319-24100-5_1
9. O. Kırbrıslı, A.E. Ersundu, M. Çelikkıle Ersundu, Dy³⁺ doped tellurite glasses for solid-state lighting: An investigation through physical, thermal, structural and optical spectroscopy studies. *J. Non-Cryst. Solids* **513**, 125–136 (2019). <https://doi.org/10.1016/j.jnoncrysol.2019.03.020>
10. V.A.G. Rivera, F.A. Ferri, L.A.O. Nunes, E. Marega Jr., White light generation via up-conversion and blue tone in Er³⁺/Tm³⁺/Yb³⁺-doped zinc-tellurite glasses. *Opt. Mater.* **67**, 25–31 (2017). <https://doi.org/10.1016/j.optmat.2017.03.028>
11. M. Soltys, A. Górny, J. Pisarska, W.A. Pisarski, Lead borate glasses triply doped with Dy³⁺/Tb³⁺/Eu³⁺ ions for white emission. *Opt. Mater.* **82**, 110–115 (2018). <https://doi.org/10.1016/j.optmat.2018.05.043>
12. K. Jha, A.K. Vishwakarma, M. Jayasimhadri, D. Haranath, Multicolor and white light emitting Tb³⁺/Sm³⁺ doped zinc phosphate barium titanate glasses via energy transfer for optoelectronic device applications. *J. Alloys Compd.* **719**, 116–124 (2017). <https://doi.org/10.1016/j.jallcom.2017.05.076>
13. M. Jayasimhadri, K. Jha, B.V. Ratnam, H.J. Woo, K. Jang, A.S. Rao, D. Haranath, Single NUV band pumped PbO-GeO₂-TeO₂:Tb³⁺ yellowish green emitting glass material for tricolor white LEDs. *J. Alloys Compd.* **711**, 395–399 (2017). <https://doi.org/10.1016/j.jallcom.2017.03.252>
14. H.I. Francisco-Rodriguez, A. Lira, O. Soriano-Romero, A.N. Meza-Rocha, S. Bordignon, A. Speghini, R. Lozada-Morales, U. Caldiño, Lithium-aluminum-zinc phosphate glasses activated with Tb³⁺ and Tb³⁺/Eu³⁺ for green laser medium, reddish-orange and white phosphor applications. *Opt. Mater.* **79**, 358–365 (2018). <https://doi.org/10.1016/j.optmat.2018.04.004>
15. S. Gopi, S.K. Jose, E. Sreeja, P. Manasa, N.V. Unnikrishnan, C. Joseph, P.R. Biju, Tunable green to red emission via Tb sensitized energy transfer in Tb/Eu codoped alkali fluoroborate glass. *J. Lumin.* **192**, 1288–1294 (2017). <https://doi.org/10.1016/j.jlumin.2017.09.009>
16. T.B. de Queiroz, M.B.S. Botelho, T.S. Gonçalves, R. Dousti, A.S.S. de Camargo, New fluorophosphate glasses codoped with Eu³⁺ and Tb³⁺ as candidates for generating tunable visible light.

- J. Alloys Compd. **647**, 315–321 (2015). <https://doi.org/10.1016/j.jallcom.2015.06.066>
17. S. Loos, M. Mungra, B. Ahrens, R.L. Leonard, A. Evans, J.A. Johnson, F. Steudel, S. Schweizer, Concentration-dependent luminescence and energy transfer in Tb³⁺/Eu³⁺ doped borate and fluorozirconate glasses. *J. Lumin.* **187**, 298–303 (2017). <https://doi.org/10.1016/j.jlumin.2017.03.030>
 18. B. Kukliński, D. Wileńska, S. Mahlik, K. Szczodrowski, M. Grinberg, A.M. Klonkowski, Luminescent GeO₂–Pb–Bi₂O₃ glasses codoped with Tb³⁺ and Eu³⁺: excitation energy transfer and color chromaticity. *Opt. Mater.* **36**, 633–638 (2014). <https://doi.org/10.1016/j.optmat.2013.10.042>
 19. D. Wileńska, K. Szczodrowski, S. Mahlik, B. Kukliński, M. Grinberg, A.M. Klonkowski, White emitting phosphors based on glasses of the type 10AlF₃–10TiO₂–39PbO–30H₃BO₃–10SiO₂–xEu₂O₃–(1–x)Tb₂O₃: an energy transfer study. *J. Lumin.* **166**, 54–59 (2015). <https://doi.org/10.1016/j.jlumin.2015.05.002>
 20. F. Hu, X. Wei, S. Jiang, S. Huang, Y. Qin, Y. Chen, C.K. Duan, M. Yin, Fabrication and luminescence properties of transparent glass-ceramics containing Eu³⁺-Doped TbPO₄ nanocrystals. *J. Am. Ceram. Soc.* **98**, 464–468 (2015). <https://doi.org/10.1111/jace.13283>
 21. R. Wang, D. Zhou, J. Qiu, Y. Yang, C. Wang, Color-tunable luminescence in Eu³⁺/Tb³⁺ codoped oxyfluoride glass and transparent glass-ceramics. *J. Alloys Compd.* **629**, 310–314 (2015). <https://doi.org/10.1016/j.jallcom.2014.12.233>
 22. T.V. Bocharova, A.N. Vlasova, G.O. Karapetyan, V.G. Kuryavii, A.M. Mironov, N.O. Tagil'tseva, Local environment of Eu³⁺ and Tb³⁺ ions in fluorophosphate glasses of the Ba(PO₃)₂–MgCaSr–BaAl₂F₁₄ system. *Glass Phys. Chem.* **34**, 683–692 (2008). <https://doi.org/10.1134/S1087659608060059>
 23. K.V. Raju, S. Sailaja, C.N. Raju, B.S. Reddy, Optical characterization of Eu³⁺ and Tb³⁺ ions doped cadmium lithium aluminofluoro boro tellurite glasses. *Spectrochim. Acta A Mol. Biomol. Spectrosc.* **79**, 87–91 (2011). <https://doi.org/10.1016/j.saa.2011.02.009>
 24. D.A. Rodríguez-Carvajal, A.N. Meza-Rocha, U. Caldiño, R. Lozada-Morales, E. Alvarez, Ma.E. Zayas, Reddish-orange, neutral and warm white emissions in Eu³⁺, Dy³⁺ and Dy³⁺/Eu³⁺ doped CdO–GeO₂–TeO₂ glasses. *Solid State Sci.* **61**, 70–76 (2016). <https://doi.org/10.1016/j.solidstatesciences.2016.09.009>
 25. M.S. Sadeq, H.Y. Morshidy, Effect of mixed rare-earth ions on the structural and optical properties of some borate glasses. *Ceram. Int.* **45**(15), 18327–18332 (2019). <https://doi.org/10.1016/j.ceramint.2019.06.046>
 26. R. El-Mallawany, Some physical properties of tellurite glasses, in *Tellurite glass smart materials*. ed. by R. El-Mallawany (Springer Nature, 2018), pp.8–13. https://doi.org/10.1007/978-3-319-76568-6_1
 27. G. Yankov, L. Dimowa, N. Petrova, M. Tarassov, K. Dimitrov, T. Petrov, B.L. Shivachev, Synthesis, structural and non-linear optical properties of TeO₂–GeO₂–Li₂O glasses. *Opt. Mater.* **35**, 248–251 (2012). <https://doi.org/10.1016/j.optmat.2012.08.002>
 28. A.G. Kalampounias, N.K. Nasikas, G.N. Papatheodorou, Structural investigations of the xTeO₂–(1–x)GeO₂ (x=0, 0.2, 0.4, 0.6, 0.8 and 1) tellurite glasses: A composition dependent Raman spectroscopic study. *J. Phys. Chem. Solids* **72**, 1052–1056 (2011). <https://doi.org/10.1016/j.jpcs.2011.05.016>
 29. N. Ghribi, M. Dutreilh-Colas, J.-R. Duclère, F. Gouraud, T. Chotard, R. Karray, A. Kabadou, P. Thomas, Structural, mechanical and optical investigations in the TeO₂-rich part of the TeO₂–GeO₂–ZnO ternary glass system. *Solid State Sci.* **40**, 20–30 (2015). <https://doi.org/10.1016/j.solidstatesciences.2014.12.009>
 30. M. Lesniak, J. Zeid, B. Starzyk, M. Kochanowicz, M. Kuwik, J. Zmojda, P. Miluski, A. Baranowska, J. Dorosz, W. Pisarski, J. Pisarska, D. Dorosz, Investigation of the TeO₂/GeO₂ ratio on the spectroscopic properties of Eu³⁺-doped oxide glasses for optical fiber application. *Materials* **15**, 117 (2022). <https://doi.org/10.3390/ma15010117>
 31. H.A.A. Sidek, S. Rosmawati, Z.A. Talib, M.K. Halimah, W.M. Daud, Synthesis and Optical Properties of ZnO–TeO₂ Glass System. *Am. J. Appl. Sci.* **6**, 1489–1494 (2009). <https://doi.org/10.3844/ajassp.2009.1489.1494>
 32. N.S. Tagiara, D. Palles, E.D. Simandiras, V. Psycharis, A. Kyritsis, E.I. Kamitsos, Synthesis, thermal and structural properties of pure TeO₂ glass and zinc-tellurite glasses. *J. Non-Cryst. Solids* **457**, 116–125 (2017). <https://doi.org/10.1016/j.jnoncrysol.2016.11.033>
 33. A. Gulenko, O. Masson, A. Berghout, D. Hamani, P. Thomas, Atomistic simulations of TeO₂-based glasses: interatomic potentials and molecular dynamics. *Phys. Chem. Chem. Phys.* **16**, 14150–14160 (2014). <https://doi.org/10.1039/c4cp01273a>
 34. M.E. Alvarez-Ramos, R.C. Carrillo-Torres, R. Sánchez-Zeferino, U. Caldiño, J. Alvarado-Rivera, Co-emission and energy transfer of Sm³⁺ and/or Eu³⁺ activated zinc-germanate-tellurite glass as a potential tunable orange to reddish-orange phosphor. *J. Non-Cryst. Solids* **521**, 119462 (2019). <https://doi.org/10.1016/j.jnoncrysol.2019.119462>
 35. I.V. García-Amaya, Ma.E. Zayas, J. Alvarado-Rivera, M. Cortez-Valadez, M. Pérez-Tello, N. Cayetano-Castro, F. Martínez-Suárez, A. Mendoza-Córdova, Influence of Eu₂O₃ on phase crystallization and nanocrystals formation in tellurite glasses. *J. Non-Cryst. Solids* **499**, 49–57 (2018). <https://doi.org/10.1016/j.jnoncrysol.2018.07.018>
 36. G. Monteiro, L.F. Santos, J.C.G. Pereira, R.M. Almeida, Optical and spectroscopic properties of germanotellurite glasses. *J. Non-Cryst. Solids* **350**, 2695–2701 (2011). <https://doi.org/10.1016/j.jnoncrysol.2010.12.062>
 37. J. Alvarado-Rivera, D.A. Rodríguez-Carvajal, M.C. Acosta-Enriquez, M.B. Manzanares-Martínez, E. Álvarez, R. Lozada-Morales, G.C. Díaz, A. de León, Ma.E. Zayas, Effect of CeO₂ on the glass structure of sodium germanate glasses. *J. Am. Ceram. Soc.* **97**, 3494–3500 (2014). <https://doi.org/10.1111/jace.13202>
 38. R.C. Carrillo-Torres, G. Saavedra-Rodríguez, J. Alvarado-Rivera, U. Caldiño, R. Sánchez-Zeferino, M.E. Alvarez-Ramos, Tunable emission and energy transfer in TeO₂–GeO₂–ZnO and TeO₂–GeO₂–MgCl₂ glasses activated with Eu³⁺/Dy³⁺ for solid state lighting applications. *J. Lumin.* **212**, 116–125 (2019). <https://doi.org/10.1016/j.jlumin.2019.04.008>
 39. K. Binnemans, Interpretation of europium (III) spectra. *Coord. Chem. Rev.* **295**, 1–45 (2015). <https://doi.org/10.1016/j.ccr.2015.02.015>
 40. W. Stambouli, H. Elhouichet, B. Gelloz, M. Ferid, Optical and spectroscopic properties of Eu-doped tellurite glasses and glass ceramics. *J. Lumin.* **138**, 201–208 (2013). <https://doi.org/10.1016/j.jlumin.2013.01.019>
 41. K. Maheshvaran, P.K. Veeran, K. Marimuthu, Structural and optical studies on Eu³⁺ doped boro-tellurite glasses. *Solid State Sci.* **17**, 54–62 (2013). <https://doi.org/10.1016/j.solidstatesciences.2012.11.013>
 42. G. Blasse, B.C. Grabmaier, *Luminescent Materials*, 1st edn. (Springer-Verlag, Berlin, 1994), pp.71–107
 43. V. Lavín, U.R. Rodríguez-Mendoza, I.R. Martín, V.D. Rodríguez, Optical spectroscopy analysis of the Eu³⁺ ions local structure in calcium diborate glasses. *J. Non-Cryst. Solids* **319**, 200–216 (2003). [https://doi.org/10.1016/S0022-3093\(02\)01914-2](https://doi.org/10.1016/S0022-3093(02)01914-2)
 44. N. Wada, K. Kojima, Glass composition dependence of Eu³⁺ ion red fluorescence. *J. Lumin.* **126**, 53–62 (2007). <https://doi.org/10.1016/j.jlumin.2006.05.002>
 45. U. Caldiño, E. Álvarez, A. Speghini, M. Bettinelli, New greenish-yellow and yellowish-green emitting glass phosphors: Tb³⁺/Eu³⁺

- and $Ce^{3+}/Tb^{3+}/Eu^{3+}$ in zinc phosphate glasses. *J. Lumin.* **135**, 216–220 (2013). <https://doi.org/10.1016/j.jlumin.2012.10.013>
46. M.R. Dousti, R.J. Amjad, Spectroscopic properties of Tb^{3+} -doped lead zinc phosphate glass for green solid state laser. *J. Non-Cryst. Solids* **420**, 21–25 (2015). <https://doi.org/10.1016/j.jnoncrsol.2015.04.002>
47. A.-B.F.A. Mohammed, G. Lakshminarayana, S.O. Baki, Kh.A. Bashar, I.V. Kityk, M.A. Mahdi, Optical and dielectric studies for Tb^{3+}/Sm^{3+} codoped borate glasses for solid-state lighting applications. *Opt. Mater.* **86**, 387–393 (2018). <https://doi.org/10.1016/j.optmat.2018.10.033>
48. N. Deop, A.S. Rao, Spectroscopic studies of single near ultraviolet pumped Tb^{3+} doped lithium lead alumino borate glasses for green lasers and tricolour w-LEDs. *J. Lumin.* **194**, 56–63 (2018). <https://doi.org/10.1016/j.jlumin.2017.09.057>
49. E. Álvarez, M.E. Zayas, J. Alvarado-Rivera, F. Félix-Domínguez, R.P. Duarte-Zamorano, U. Caldiño, New reddish-orange and greenish-yellow light emitting phosphors: Eu^{3+} and Tb^{3+}/Eu^{3+} in sodium germanate glass. *J. Lumin.* **153**, 198–202 (2014). <https://doi.org/10.1016/j.jlumin.2014.03.031>
50. M.E. Alvarez-Ramos, J. Alvarado-Rivera, M.E. Zayas, U. Caldiño, J. Hernández-Paredes, Yellow to orange-reddish glass phosphors: Sm^{3+} , Tb^{3+} and Sm^{3+}/Tb^{3+} in zinc tellurite-germanate glasses. *Opt. Mater.* **75**, 88–93 (2018). <https://doi.org/10.1016/j.optmat.2017.09.033>
51. M. Inokuti, F. Hirayama, Influence of energy transfer by the exchange mechanism on donor luminescence. *J. Chem. Phys.* **43**, 1978–1989 (1965). <https://doi.org/10.1063/1.1697063>
52. A.U. Trápala-Ramírez, J.L.N. Gálvez-Sandoval, A. Lira, I. Camarillo, M.E. Álvarez-Ramos, A.N. Meza-Rocha, U. Caldiño, Calcium-zinc phosphate glasses activated with Tb^{3+}/Eu^{3+} for laser and white LED applications. *J. Lumin.* **215**, 116621 (2019). <https://doi.org/10.1016/j.jlumin.2019.116621>
53. M.E. Álvarez-Ramos, Study of the optical properties and cross relaxation process of Dy^{3+} under simultaneous UV-IR excitation in tellurite glasses. *J. Lumin.* **233**, 117874 (2021). <https://doi.org/10.1016/j.jlumin.2020.117874>
54. C.S. McCamy, Correlated color temperature as an explicit function chromaticity coordinates. *Color. Res. Appl.* **17**, 142–144 (1992). <https://doi.org/10.1002/col.5080170211>

Publisher's Note Springer Nature remains neutral with regard to jurisdictional claims in published maps and institutional affiliations.

Springer Nature or its licensor (e.g. a society or other partner) holds exclusive rights to this article under a publishing agreement with the author(s) or other rightsholder(s); author self-archiving of the accepted manuscript version of this article is solely governed by the terms of such publishing agreement and applicable law.